The application of repro-modelling to pyrocarbon CVD/CVI homogeneous mechanisms for various hydrocarbons precursors

A. Mouchon [a)], G.L. Vignoles [a)] and F. Langlais [a)]
a) Laboratoire des Composites Thermostructuraux, 3 allée de la Boëtie, F-33600 Pessac, France

ABSTRACT

The pyrocarbon Chemical Vapor Infiltration (CVI) is a widespread process for the production of high-performance composite materials with applications in aerospace and braking technology. Several hundred species and thousands of elementary reactions may be required to describe comprehensively the gas-phase pyrolysis that occurs prior to pyrocarbon deposition. The repro-modelling technique is a well suited reduction method of such a large chemical reaction mechanism. Chemical kinetics are described as explicit functional relations between the source terms and the concentrations of related species, obtained by fitting the numerical solution of differential equations. The reduction procedure consists in a parameterization based on orthonormal polynomials.

This technique has been applied to zero and one-dimensional simulations of a global model for pyrolysis of methane, propane and propylene. These simulations were performed in different conditions of pressure, temperature and residence time of the precursor. The approximations of species concentration profiles are in good agreement with the original numerical data and with experimental data, thus providing a new insight in the understanding of pyrocarbon deposition.

INTRODUCTION

Carbon/carbon (C/C) composite materials are used in a variety of high-temperature structural applications such as rocket propeller nozzles, heat shields for re-entry vehicles and aircraft brake discs. C/C composites are mainly produced by chemical vapor deposition/ chemical vapor infiltration (CVD/CVI) processes, in which a preform made of carbon fibers is densified by a pyrocarbon (PyC) deposit originated in the cracking of gaseous hydrocarbons.

Pyrolytic carbon is known to exhibit a broad variety of microstructures in the context of CVD and/or CVI [1,2], ranging from nearly isotropic to highly anisotropic (*i.e.* close to graphite structure). Among them, two varieties, called “Rough Laminar” (RL, also denoted as *high-textured*) and “Smooth Laminar” (SL, also denoted as *medium-or low-textured*) because of their appearances when imaged by Polarized Light Optical Microscopy (PLOM), differ by their degree of structural anisotropy, and have distinct mechanical and optical properties. Furthermore, only the RL form is graphitizable by a high-temperature post-treatment [2,3].

A key issue in PyC CVD/CVI is the control of the deposit microstructure during the infiltration, which depends on processing parameters such as temperature T, pressure p and composition ratios, as well as residence time t_R and surface-to-volume ratio S_v

[4-6]. The nature of the hydrocarbon precursor is also a key point, as it may alter strongly the gas-phase composition and reactivity.

The hydrocarbon pyrolysis, which precedes the PyC deposition, follows a long chain of homogeneous reactions in a so-called “maturation” process [7], where several hundred species and thousands of elementary reactions may be required to describe the chemical mechanism comprehensively. The successive steps are : (*i*) a cracking of the initial molecules into more reactive and lighter gaseous species, (*ii*) a recombination of these species into light aromatic compounds, and (*iii*) an evolution of these aromatic compounds (among which PAHs – Polycylic Aromatic Hydrocarbons) towards higher molecular weights in a polymerization-like reaction.

The PyC deposit may originate from both light and heavy hydrocarbons, probably with distinct mechanisms: heavy hydrocarbons are thought to deposit in a condensation-like mechanism [8,9], while, for light species, a lateral growth mechanism, close to a polymerization reaction scheme, has been proposed [10]. Several models have been established to explicit the nature of the PyC precursors and the deposition process.

Comprehensive gas-phase models have been developed in the case of methane decomposition [11] and of nanotube CVD [12]. A global model has also been set up for PyC deposition from propane pyrolysis [13]. It has been checked by correlation with Fourier-transform-infrared (FTIR) gas-phase analyses and with deposit nanotexture and growth rate characterizations.

The introduction of these models in realistic 2D and 3D computations cannot be made using comprehensive homogeneous mechanisms because of the computational burden. The reduction of large detailed mechanisms into smaller ones is therefore a key point. A reduction method proposed in this paper is the description of chemical kinetics by explicit functions, which are sums of orthogonal polynomials, the parameters of which are obtained by numerical fitting to the computed solution of differential equations describing the extensive mechanism [14].

In the first part of this paper, we will present the main results for ØD and 1D computations of pyrolysis using propane, methane and propylene as precursors, and correlate these results with experimental data when available. Then, the repro-modelling technique will be briefly presented, followed by its application to some cases of the previously mentioned ØD and 1D computations. The results of the parameterization process will be compared to those of the detailed mechanism for some key species and the interest of such a computational tool will be discussed in the frame of PyC deposition.

1/ ØD AND 1D COMPUTATIONS USING GLOBAL MODELS

ØD and 1D computations have been performed in the modelling of propane, methane and propylene pyrolysis in different conditions of pressure, temperature and residence time summarized in table 1. The *Senkin* software (Chemkin Package, Sandia Laboratories) has been used for ØD simulations, and 1D simulations have been performed using a homemade 1D solver with finite volume discretization [15].

Precursor	ØD simulations	1D simulations
Propane	- P = 2kPa - T from 950 to 1300K	- P from 0.5 to 5kPa - T = 1223K - t_R from 5.10^{-4} to 2s
Methane + Argon		- Partial pressure 10kPa/ total pressure 100kPa - T = 1373K - t_R from 5.10^{-2} to 1s
Propylene + Argon		- Partial pressure 4kPa/ total pressure 100kPa - T = 1273K - t_R from 5.10^{-2} to 1s

Table 1. Conditions of pyrolysis for ØD and 1D computations

The kinetic mechanisms used in these simulations are a compilation of numerous kinetic databases (e.g. [15-17]), most of them arising from combustion examples. This mechanism includes molecular hydrocarbon species, up to naphtalene $C_{10}H_8$, as well as the associated resonance-stabilized free radical species (RSFRs).

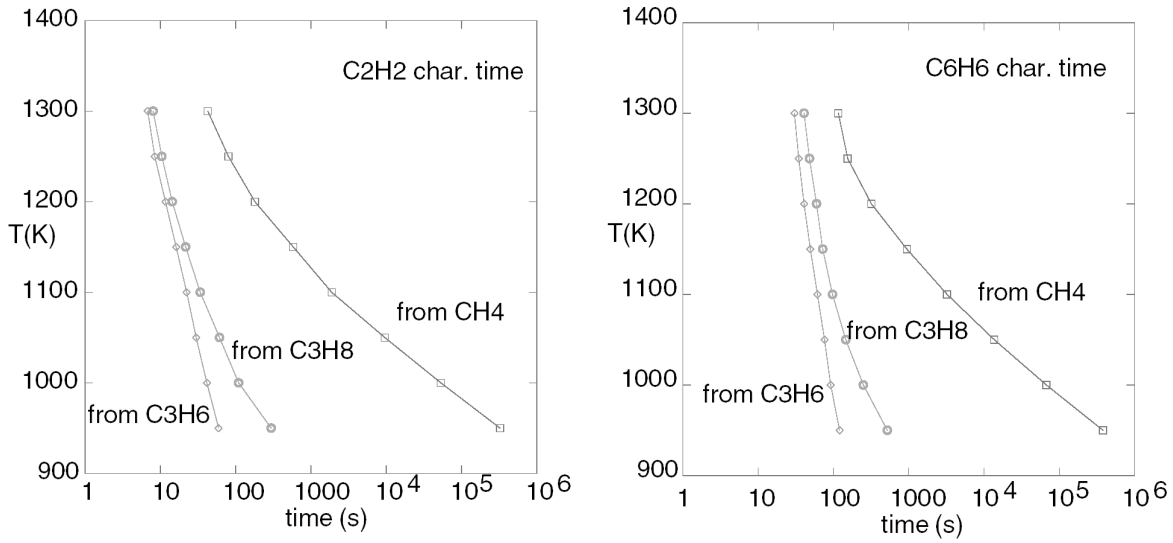

Figure 1. Characteristic time for C_2H_2 and C_6H_6 production from C_3H_8, CH_4 and C_3H_6

An illustration of the ØD computations is reported on figure 1, considering all the mentioned precursors in the same conditions of pyrolysis [P=2kPa, T ranging from 950 to 1300K and all pure precursors]. The time profiles of C_2H_2 and C_6H_6 have been computed [13], and the characteristic time of appearance for these species has been drawn as a function of temperature.

As propylene is one of the first by-products of propane decomposition, it leads to a shift of C_2H_2 and C_6H_6 characteristic times towards lower values, especially at low temperatures. On the other hand, using methane leads to a shift towards high residence times, thus confirming the well-known lower methane reactivity, which implies a long induction period before yielding appreciable amounts of reaction intermediates like unsaturated C2 species.

1D computations have been performed for each precursor and compared to FTIR data for propane [18,19] and gas-phase chromatography (GPC) analysis for methane and propylene [20,21]. To illustrate the propane case, experimental data (resulting from FTIR signal integration along the CVD hot-wall reactor) and calculated outlet scaled partial pressures have been drawn for several species on figure 2 as a function of residence time for *P*=0,5kPa. The evolution of the calculated partial pressures are in good qualitative agreement with experimental data, although there is a shift due to thermal effects for some species which exhibit a maximum, e. g. towards lower residence times for C_3H_6 and towards higher values for propyne. The difference for the propane evolution is related to the FTIR integration, which also includes the cold part of the reactor where the precursor decomposition is partial.

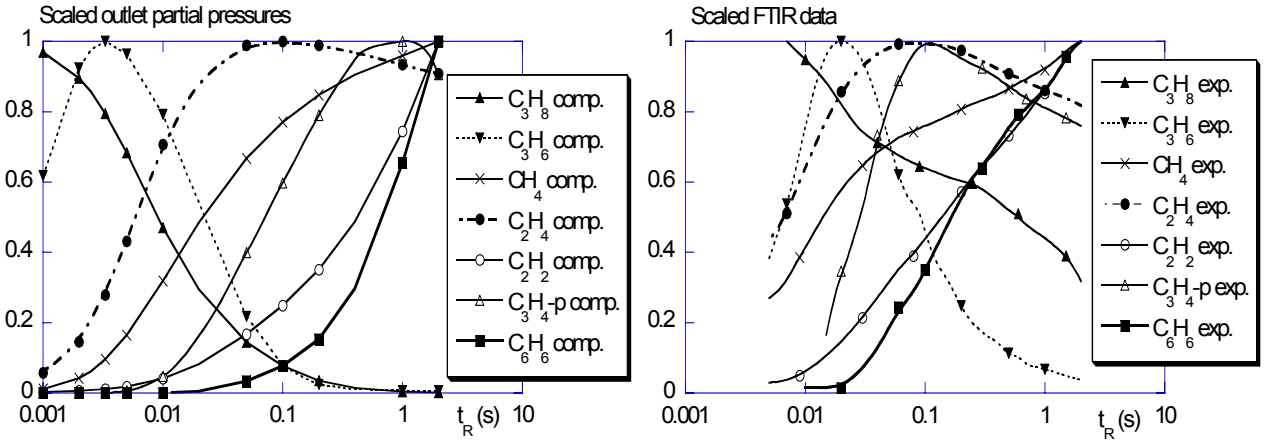

Figure 2. Computed and experimental gas-phase species time evolution [pure propane *P*=0,5kPa]

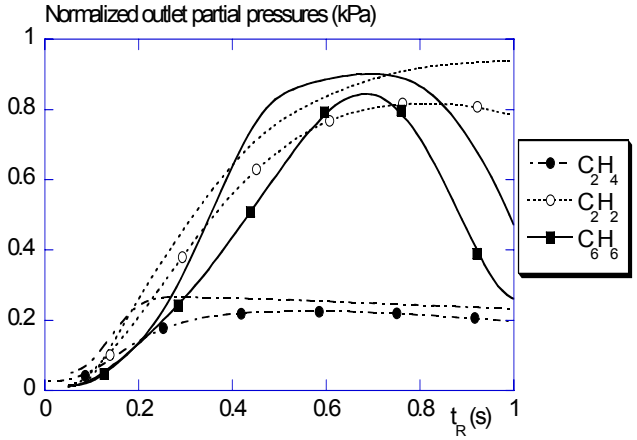

Figure 3. C_2H_4 , C_2H_2 and C_6H_6 time evolution with CH_4 precursor [initial p.p. 10kPa, *T*=1373K]

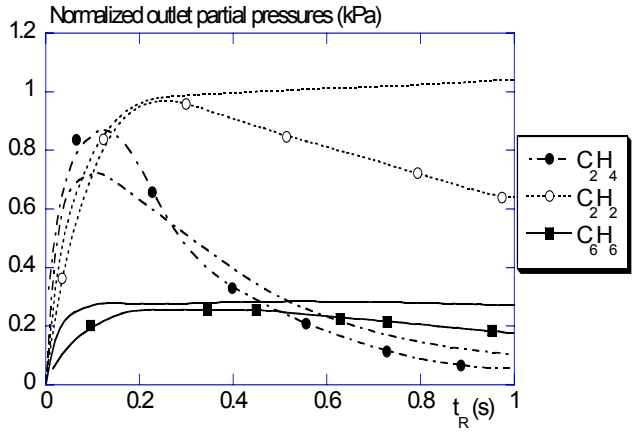

Figure 4. C_2H_4 , C_2H_2 and C_6H_6 time evolution with C_3H_6 precursor [initial p.p. 4kPa, *T*=1273K]

[lines with markers stand for data, lines for comp.]

Figure 3 and figure 4 show the residence time profiles for C_2H_4, C_2H_2 and C_6H_6 in the methane and propylene cases respectively. The computational results can be directly compared to the experimental ones (GPC) as normalized outlet partial pressures are provided. The differences observed for C_2H_2 and C_6H_6 time profiles are related to the fact that heterogeneous reactions, where C_2H_2 and C_6H_6 may act, are not taken into account in those models. However, the tendencies are quite well reproduced for each species. The homogeneous mechanisms built up in this study for each precursor seem therefore to be consistent as they are validated by experimental data.

2/ METHODOLOGY OF THE REPRO-MODELLING TECHNIQUE

Most of reduction methods in chemical kinetics have been developed in combustion issues, which necessitate lengthy computations because of the high number of species involved (leading to the same number of equations to solve) and because of the various time scales (responsible for the numerical stiffness). These methods can be divided into two groups, whether they are based on time-scale analysis or not [22]. The repro-modelling technique is not based on time scale analysis but involves fitting multivariate polynomials to a dataset that is representative of the chemical system.

The repro-modelling technique was applied successfully to a combustion case by Turányi [23] but also to atmospheric chemistry [24,25] or to an oscillating reaction such as the Oregonator model of the Belousov-Zhabotinsky reaction [14]. Turányi developed a method for generating high-order polynomials using an orthonormal basis set [14], and this is the method that is used here.

A polynomial is generated for each of the key species of the system to represent the change in concentration of that species from one time point to the next. The variables of the repro-model must therefore include not only the key species but also any physical parameters that affect species concentrations such as temperature, or pressure. These variables are called the *basic variables* ($X_1, X_2, \ldots X_m$) and it is an essential part of the procedure to develop a dataset of dimension *m* that is large enough to represent the system but not too large for obvious practical reasons. The smaller the number of variables, the simpler and the computationally faster the approximating function is.

Once the *m*-dimensional dataset is created, the polynomials are calculated using the Gram-Schmidt orthonormalisation procedure.

Any function *F* can be approximated using an orthonormal set of functions ($\alpha_1, \alpha_2, \ldots \alpha_l$) by an orthonormal Fourier expansion:

$$F \approx \sum_{j=1}^{l} \left\langle F, \alpha_j \right\rangle \alpha_j \tag{1}$$

where functions are defined as orthonormal if and only if the scalar product :

$$\begin{aligned} \left\langle \alpha_j, \alpha_k \right\rangle &= 0 \; if \;\; j \neq k \\ \left\langle \alpha_j, \alpha_k \right\rangle &= 1 \; if \;\; j = k \end{aligned} \tag{2}$$

The accuracy of the fitted function can be calculated as a root mean square error (r.m.s) *r* :

$$r = \left\| F - \sum_{j=1}^{l} \left\langle F, \alpha_j \right\rangle \alpha_j \right\| \tag{3}$$

where $\| \ \|$ is the euclidian norm.

The orthonormal functions are calculated from linear combinations of the *m* basic variables included in the dataset by using the Gram-Schmidt procedure. A weighting function w_i, i =1,..,n, is used to ensure the same accuracy of the approximation for both high and low concentrations :

$$w_i = \frac{1}{F^2(x_j^i)} \tag{4}$$

where x_j^i is the concentration of variable X_j at point *i*, n is the number of data points.

Each polynomial is generated by first fitting a constant to the data and calculating the r.m.s. error from Eq. (3). A new term is then added, an orthonormal polynomial is generated and the new r.m.s error is calculated. This term is accepted if the reduction in r.m.s error is greater than a preset tolerance, or discarded if not, and a new term is tested. By this way, the multivariate polynomial is built up with terms of progressively increasing order – from first-order terms in each variable to typically fourth - or fifth-order terms in combinations of variables. When all the possible terms have been tested and the final orthonormal polynomial has been accepted, this polynomial is converted back in the terms of the original variables of the dataset.

3/ APPLICATION OF THE REPRO-MODELLING TO ØD AND1D SIMULATIONS

As an illustration of the potentiality of the repro-modelling technique, applications to ØD simulations from propane and methane, and to 1D simulations from propane only will be presented in this part. The basic variables chosen in this study are species of interest, present in relatively important amounts in the gas-phase. In the propane case these species are : C_3H_8, C_3H_6, CH_4, C_2H_2, C_2H_4 and C_6H_6 ; and in the methane case : CH_4, C_2H_2, C_2H_4, C_2H_6 and C_6H_6. The maximum order of the polynomials is limited to 3 in order to diminish the amount of data to be generated and the following applications show that this value is relevant.

Figure 5 demonstrates the remarkably good agreement between the C_2H_4 time evolution given by the detailed mechanism in ØD simulations (*T*=1000K for C_3H_8 and 1300K for CH_4) and by the repro-model for both precursors (standard deviation of 1.5% for CH_4 and 3% for C_3H_8). The plots drawn on figure 6 (C_3H_8 pure precursor with *P*=0.5kPa), representing the time evolution for C_3H_8, CH_4 and C_2H_4 outlet molar fractions, also exhibit the weak differences between profiles given by 1D computations

and given by the repro-model (standard deviation of 1.92% for C_3H_8, 0.72% for CH_4 and 0.6% for C_2H_4).

These few examples presented here clearly show the interest of repro-modelling as an efficient computational tool to reduce detailed gas-phase pyrolysis mechanisms.

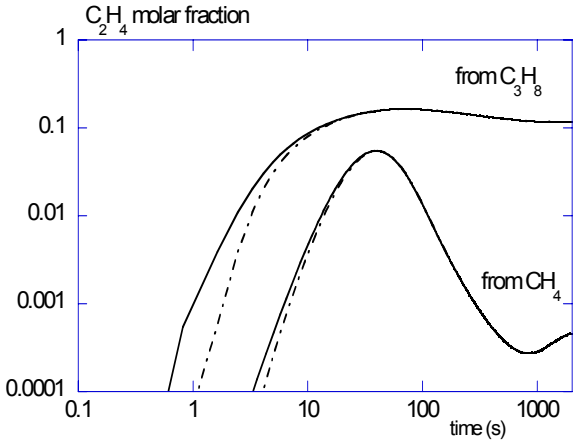

Figure 5. ØD C_2H_4 molar fraction time evolution

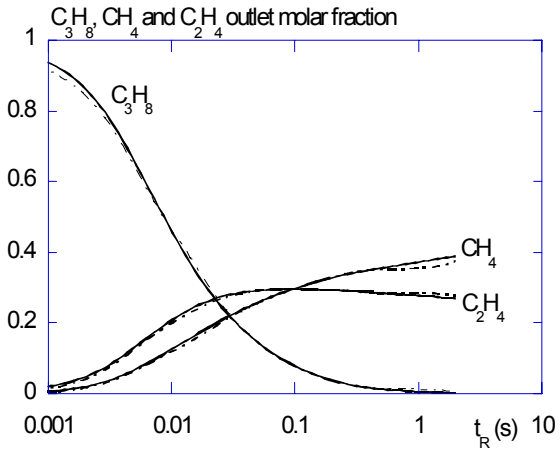

Figure 6. 1D C_3H_8, CH_4 and C_2H_4 molar fraction time evolution [C_3H_8 precursor, *P*=0.5kPa]

[plain lines stand for detailed model, dotted lines for repro-model]

4/ CONCLUSION

The application of the repro-modelling method to detailed CVD/CVI homogeneous mechanisms has been described in this paper. This technique has provided a successful parameterization of global pyrolysis models in the physicochemical conditions of interest in the application. It is the aim of a future work to implement the parametric models thus obtained into realistic 2D and 3D modellings of CVD and CVI furnaces, including heterogeneous mechanisms. This should lead to a better understanding of the PyC deposition process, and particularly of the nature of the ultimate PyC precursors for the various PyC nanotextures.

ACKNOWLEDGEMENTS

The authors wish to acknowledge the support of Centre National de la Recherche Scientifique and Snecma Propulsion Solide through a Ph. D. grant to A M. The authors also thank C. Descamps (Snecma Propulsion Solide) for helpful discussions.

REFERENCES

[1] JC Bokros. Chemistry and Physics of Carbon 5 (1969) 1.
[2] P Loll, P Delhaès, A Pacault and A Pierre. Carbon 15 (1977) 383.
[3] A Oberlin. Carbon 22 (1984) 521.
[4] RJ Diefendorf in JW Mitchell, RC de Vries, and P Cannon (eds.). Reactivity of solids, Wiley & sons, New York (1969).
[5] P Lieberman and HO Pierson. Carbon 12 (1974) 233.
[6] A Becker and KJ Hüttinger. Carbon 36 (3) (1998) 225.
[7] P Dupel, R Pailler and F Langlais. Journal of Materials Science 29 (1994) 1341.
[8] PA Tesner. 7th Symposium on Combustion, London, Oxford 1958. Academic Press, New York (1959) 546.
[9] JC Bokros. Carbon 3 (1965) 17.
[10] M Frenklach in A. R. Burgess *et al.* (eds.). Proc. 26th Symposium (Intl.) on Combustion. The Combustion Institute, Pittsburgh (1996) 2295.
[11] WG Zhang, ZJ Hu and KJ Hüttinger. Carbon 40 (2002) 2529.
[12] N Birakayala and EA Evans. Carbon 40 (2002) 675.
[13] GL Vignoles, F Langlais, N Reuge, H Le Poche, C Descamps and A Mouchon. ECS Proceedings PV 2003-08 (2003) 144.
[14] T Túranyi. Computers Chemistry 18 (1) (1994) 45.
[15] C Descamps, GL Vignoles, O Féron, F Langlais and J Lavenac. Journal of the Electrochemical Society 148 (2001) 695.
[16] W Tsang and RF Hampson. J. Phys. Chem. Ref. Data 15 (1986) 1087.
[17] NM Marinov, WJ Pitz, CK Westbrook, MJ Castaldi and SM Senkan. Combust. Sci. Technol. 211 (1996) 116.
[18] H Le Poche. PhD thesis, Université Bordeaux 1 (2002)
[19] O Féron, F Langlais, R Naslain and J Thebault. Carbon 37 (1999) 1343.
[20] A Becker and KJ Hüttinger. Carbon 36 (3) (1998) 213.
[21] A Becker and KJ Hüttinger. Carbon 36 (3) (1998) 201.
[22] AS Tomlin, T Túranyi, MJ Pilling in Pilling, MJ (Ed.), Autoignition and Low Temperature Combustion of Hydrocarbons. Elsevier, Amsterdam (1998).
[23] T Túranyi. Proc. Combust. Inst., 25 (1995), 948-955.
[24] AM Dunker. Atmospheric Environment 20 (1986) 479.
[25] RM Lowe and AS Tomlin. Environmental Modelling & Software 15 (2000) 611.